

Implications of Eccentric Observations on Binary Black Hole Formation Channels

MICHAEL ZEVIN,^{1,2,*} ISOBEL M. ROMERO-SHAW,^{3,4} KYLE KREMER,^{5,6} ERIC THRANE,^{3,4} AND PAUL D. LASKY^{3,4}

¹*Kavli Institute for Cosmological Physics, The University of Chicago, 5640 South Ellis Avenue, Chicago, Illinois 60637, USA*

²*Enrico Fermi Institute, The University of Chicago, 933 East 56th Street, Chicago, Illinois 60637, USA*

³*School of Physics and Astronomy, Monash University, Vic 3800, Australia*

⁴*OzGrav: The ARC Centre of Excellence for Gravitational Wave Discovery, Clayton VIC 3800, Australia*

⁵*TAPIR, California Institute of Technology, Pasadena, CA 91125, USA*

⁶*The Observatories of the Carnegie Institution for Science, Pasadena, CA 91101, USA*

ABSTRACT

Orbital eccentricity is one of the most robust discriminators for distinguishing between dynamical and isolated formation scenarios of binary black holes mergers using gravitational-wave observatories such as LIGO and Virgo. Using state-of-the-art cluster models, we show how selection effects impact the detectable distribution of eccentric mergers from clusters. We show that the observation (or lack thereof) of eccentric binary black hole mergers can significantly constrain the fraction of detectable systems that originate from dynamical environments such as dense star clusters. After roughly 150 observations, observing no eccentric binary signals would indicate that clusters cannot make up the majority of the merging binary black hole population in the local Universe (95% credibility). However, if dense star clusters dominate the rate of eccentric mergers and a single system is confirmed to be measurably eccentric in the first and second gravitational-wave transient catalogues, clusters must account for at least 14% of detectable binary black hole mergers. The constraints on the fraction of detectable systems from dense star clusters become significantly tighter as the number of eccentric observations grows, and will be constrained to within 0.5 dex once 10 eccentric binary black holes are observed.

1. INTRODUCTION

In the past few years, the dramatic increase in compact binary mergers observed by gravitational-wave (GW) detectors has fueled immense interest and debate regarding compact binary formation pathways, particularly for binary black hole (BBH) systems. Over a dozen potential formation scenarios for the BBH mergers observed by the LIGO–Virgo detector network (Aasi et al. 2015; Acernese et al. 2015) have been proposed, including isolated massive-star binary progenitors (e.g., Bethe & Brown 1998; Dominik et al. 2012; Belczynski et al. 2016; Bavera et al. 2021), assembly in dynamical environments (e.g., Portegies Zwart & McMillan 2000; O’Leary et al. 2006; Downing et al. 2010; Rodriguez et al. 2016; Banerjee 2017; Di Carlo et al. 2019), gas-driven assembly and orbital evolution (e.g., McKernan et al. 2014; Bartos et al. 2017; Stone et al. 2017), and primordial origins (e.g., Bird et al. 2016; Sasaki et al. 2018; Clesse & Garcia-Bellido 2020; Franciolini et al. 2021).

Given the heterogeneity of compact binary coalescences observed to date, a mix of formation channels is currently preferred over one single channel dominating the formation of merging BBH systems in the Universe (Abbott et al. 2020a; Zevin et al. 2021; Wong et al. 2021; Bouffanais et al. 2021).

Though population-based studies offer insights into the broad features of BBH formation, the most efficient means of constraining formation scenarios is to identify features of BBH systems unique to particular channels. One such key feature is orbital eccentricity. Compact binary systems that inspiral over long timescales efficiently damp orbital eccentricity through angular momentum loss from GW emission (Peters 1964). Therefore, even field binaries born with high eccentricity are nearly circular by the time they enter the LIGO–Virgo sensitive frequency band. For example, a BBH composed of two $20 M_{\odot}$ black holes (BHs) at an initial orbital separation of $1 R_{\odot}$ and initial eccentricity of 0.9 (0.99) will have an eccentricity at a GW frequency of 10 Hz of 0.001 (0.05) and merge in 32 yr (6 day). The only means of producing measurably eccentric BBH mergers in the LIGO–Virgo band that does not require a high

degree of fine-tuning is through strong gravitational encounters in dynamical environments (e.g., O’Leary et al. 2009; Kocsis & Levin 2012; Samsing et al. 2014; Rodriguez et al. 2018b; Samsing et al. 2018; Samsing 2018; Takatsy et al. 2019; Zevin et al. 2019; Gondán & Kocsis 2020; Gröbner et al. 2020; Samsing et al. 2020b; Tagawa et al. 2021) or through channels that can pump eccentricity into inspiraling binaries, such as the secular evolution of hierarchical systems (e.g., Antonini & Perets 2012; Antognini et al. 2014; Silsbee & Tremaine 2017; Antonini et al. 2017; Rodriguez & Antonini 2018; Fragione & Bromberg 2019; Fragione & Kocsis 2019; Liu & Lai 2019).

Orbital eccentricity is also arguably the most robust discriminator for distinguishing between isolated and dynamical BBH formation scenarios; so long as BHs form in clusters and are not kicked out of clusters at formation, highly-eccentric mergers are an inevitable byproduct of two-body relaxation and small- N dynamics (Samsing et al. 2014; Rodriguez et al. 2018b). In classical globular clusters (GCs), which are perhaps the best-studied environment of eccentric mergers from strong gravitational encounters, the presence of BHs is evidenced both observationally (through detection of BH binary candidates in several Milky Way GCs; Strader et al. 2012; Giesers et al. 2018, 2019) and computationally through N -body modeling (Mackey et al. 2007; Breen & Heggie 2013; Wang et al. 2016; Kremer et al. 2018, 2019; Arca Sedda et al. 2018; Antonini & Gieles 2020; Weatherford et al. 2020; Kremer et al. 2020). Eccentric mergers from strong gravitational encounters have been shown both semi-analytically and numerically to account for $\approx 10\%$ of the underlying population of BBH mergers in globular clusters, with approximately half of these having eccentricities $\gtrsim 0.1$ at a GW frequency of 10 Hz, the lower edge of the LIGO–Virgo band (Samsing & Ramirez-Ruiz 2017; Samsing et al. 2018; Samsing 2018; Rodriguez et al. 2018b; Zevin et al. 2019; Kremer et al. 2020).

Despite the robust theoretical predictions for forming eccentric BBH systems in clusters, the implications that such a detection would have on constraining BBH formation scenarios depends sensitively on the interplay between the *measurability* and *detectability* of such systems. Eccentricity acts as a double-edged sword: larger eccentricities are easier to distinguish from their circular counterparts using parameter estimation, though there is an inherent selection bias impinging the detection of eccentric sources due to the template banks used for matched-filter searches for GW signals, which assume quasi-circular aligned-spin binaries (Hooper et al. 2012; Allen et al. 2012; Dal Canton et al. 2014; Usman et al.

2016; Adams et al. 2016; Messick et al. 2017; Nitz et al. 2017; Chu et al. 2020; Davies et al. 2020; Aubin et al. 2021). Though burst searches may be used to detect unmodeled sources such as highly-eccentric mergers (Tiwari et al. 2016; Abbott et al. 2019a; Ramos-Buades et al. 2020), they are less capable of digging deep into the noise for signals and their sensitivity is more difficult to quantify (Klimenko et al. 2016). In terms of measurability, BBH systems with properties similar to GW150914 (Abbott et al. 2016) can be distinguished as eccentric if their eccentricities are $\gtrsim 0.05$ at a GW frequency of 10 Hz (Lower et al. 2018), consistent with the upper limits on orbital eccentricity (Romero-Shaw et al. 2019) for the events in the first LIGO–Virgo GW transient catalog (GWTC-1; Abbott et al. 2019b).¹ However, even if an eccentric GW source were detected, there is currently no published selection function for eccentric sources to translate this detection into characteristics about the source population, such as the merger rate. This is in part because of the difficulty in modeling eccentric signals (Loutrel 2020) and the computational burden of adding an extra dimension to matched-filter template banks.

In this Letter, we quantify how the detection of an eccentric BBH merger (or lack thereof) impacts the inferred fraction of BBH mergers originating from dense stellar clusters² by approximating selection effects that account for eccentricity in a realistic cluster population. With selection effects and measurability of eccentric sources accounted for, the robustness of eccentricity predictions from cluster modeling allows for constraints to be placed on the relative contribution of BBH mergers from clusters. In Section 2 we describe the cluster models used as a basis in this analysis. Section 3 covers the determination of selection effects for generically eccentric systems and our assumptions regarding the ability of eccentric sources to be distinguished from circular. Our main results are presented in Section 4, which quantifies the constraints that a bona fide eccentric detection will

¹ There are claims that an eccentric BBH merger has been observed in the most recent observing run (GW190521; Romero-Shaw et al. 2020; Gayathri et al. 2020), although this interpretation is speculative. We discuss this further in Sections 4 and 5.

² We use the term “dense star clusters” to denote clusters with masses in the range $\approx 10^5 - 10^7 M_\odot$ and virial radii of $\approx 0.5 - 5$ pc. Critically however, we do not limit this definition to only old low-metallicity clusters that survive to present day like traditional GCs. We incorporate also high-metallicity clusters born relatively recently (essential for producing lower-mass BH mergers, Chatterjee et al. 2017) as well as disrupted clusters that do not survive to the present day (inclusion of these disrupted clusters may increase the total BBH merger rate from clusters by a factor of ≈ 2 ; e.g., Rodriguez & Loeb 2018; Fragione & Kocsis 2018).

have on the contribution of dynamical channels to the underlying population of BBH systems, in the context of both the current catalogs of GWs and future observations. We summarize our results and discuss caveats of our analysis in Section 5. We use a flat Λ CDM cosmology with *Planck 2015* cosmological parameters (Ade et al. 2016) throughout this work.

2. CLUSTER MODELS

We use the dense star cluster models from the **CMC Cluster Catalog** (Kremer et al. 2020) to construct our population of dynamical BBH mergers. Collectively, these models span roughly the full parameter space of the Milky Way GCs (in cluster mass, core/half-light radius, metallicity, and position within the Galactic potential) and include state-of-the-art prescriptions for stellar evolution and black hole formation (see Kremer et al. 2020, for more details). Importantly, strong binary-mediated gravitational encounters are modeled with direct integration using *Fewbody* (Fregeau et al. 2004; Fregeau & Rasio 2007) with updates to include post-Newtonian terms for dynamical encounters involving BHs (Rodriguez et al. 2018a,b).

Gravitational radiation reaction, which enters at the 2.5 post-Newtonian order, is crucial for the formation of high-eccentricity BBH mergers in clusters (Samsing et al. 2014; Samsing & Ramirez-Ruiz 2017; Rodriguez et al. 2018b; Zevin et al. 2019). During strong gravitational encounters between single and/or binary BH systems, component BHs can undergo dozens of partner swaps, forming hardened temporary binaries that have eccentricities e drawn from a “quasi-thermal” distribution (the probability density is proportional to e). If this intermediate-state binary has a large enough orbital eccentricity, the efficient loss of orbital energy from GWs during close periastron passages leads to a rapid merger on a timescale of days with significant eccentricity in the sensitive frequency ranges of ground-based GW detectors. In addition, classically unbound BHs can lose enough orbital energy from close passages during these encounters to become bound and rapidly merge. This can also occur between two single BHs in the cluster if the impact parameter is small enough, though this subchannel produces BBH mergers with eccentricities more accessible in the deci-Hertz regime (Samsing et al. 2020a).

These merger channels from strong gravitational encounters are collectively referred to as GW captures, and have significantly larger eccentricities compared to BBH mergers that were ejected from the cluster due to a prior dynamical interaction or BBHs that merge between strong gravitational encounters (Samsing 2018;

Rodriguez et al. 2018a; Zevin et al. 2019). Figure 1 shows normalized eccentricity distributions from our cluster models at a reference GW frequency of 10 Hz, $e_{10\text{ Hz}}$, both with and without the inclusion of selection effects (described in detail in the next Section). Further details regarding the cluster population and determination of BBH eccentricities can be found in Appendix A.

3. SELECTION EFFECTS AND MEASURABILITY OF ECCENTRIC SOURCES

Due to the lack of large-scale injection campaigns that have the ability to determine sensitive space-time volume for eccentric sources, we instead estimate detection probabilities using a fixed SNR threshold required for detection. We use the waveform approximant *TEOBResumS* (Damour & Nagar 2014; Nagar et al. 2018) for all SNR calculations, which is a time-domain effective-one-body approximant (Buonanno & Damour 1999, 2000; Damour et al. 2000; Damour 2001; Damour et al. 2015) that can account for orbital eccentricity in the inspiral. *TEOBResumS* agrees well with numerical relativity (NR) for eccentricities of $e \lesssim 0.3$ at apastron frequency $\omega_a^{\text{EOB}} \sim 0.03$ (which corresponds to a GW frequency of ≈ 10 Hz for a BBH with total mass of $60 M_\odot$, Chiaramello & Nagar 2020; Albanesi et al. 2021; Nagar et al. 2021), and though untested for larger eccentricities due to a lack of available NR waveforms for comparison, is physically valid even at high eccentricities of $e_{10\text{ Hz}} \simeq 0.9$.

For each system, we calculate three separate time- and phase-maximized SNRs with different assumptions: (1) the system is circular ($e_{10\text{ Hz}} = 0$) and the template is a perfectly-matching circular template, (2) the system is eccentric with $e_{10\text{ Hz}} > 0$ and the template is a perfectly-matching eccentric template, and (3) the system is eccentric with $e_{10\text{ Hz}} > 0$ and the template is a circular template with all other source properties identical. The first two of these correspond to the “optimal SNR” in the circular and eccentric cases, respectively, while the third characterizes the loss of signal from waveform mismatch.³ In Figure 2, we show both the maximized matched-filter SNR and detection probability for an exemplary BBH system over a range of eccentricities when entering the LIGO–Virgo band. Further details on SNR calculations and determination of detection probabilities are in Appendix B.

³ A higher maximal SNR may be achieved in the third case through marginalization over intrinsic parameters of the template, making our maximal matched-filter SNRs a conservative lower limit. However, additional factors that may increase our estimated SNRs will alter results by less than a factor of 2, as discussed in Section 5.

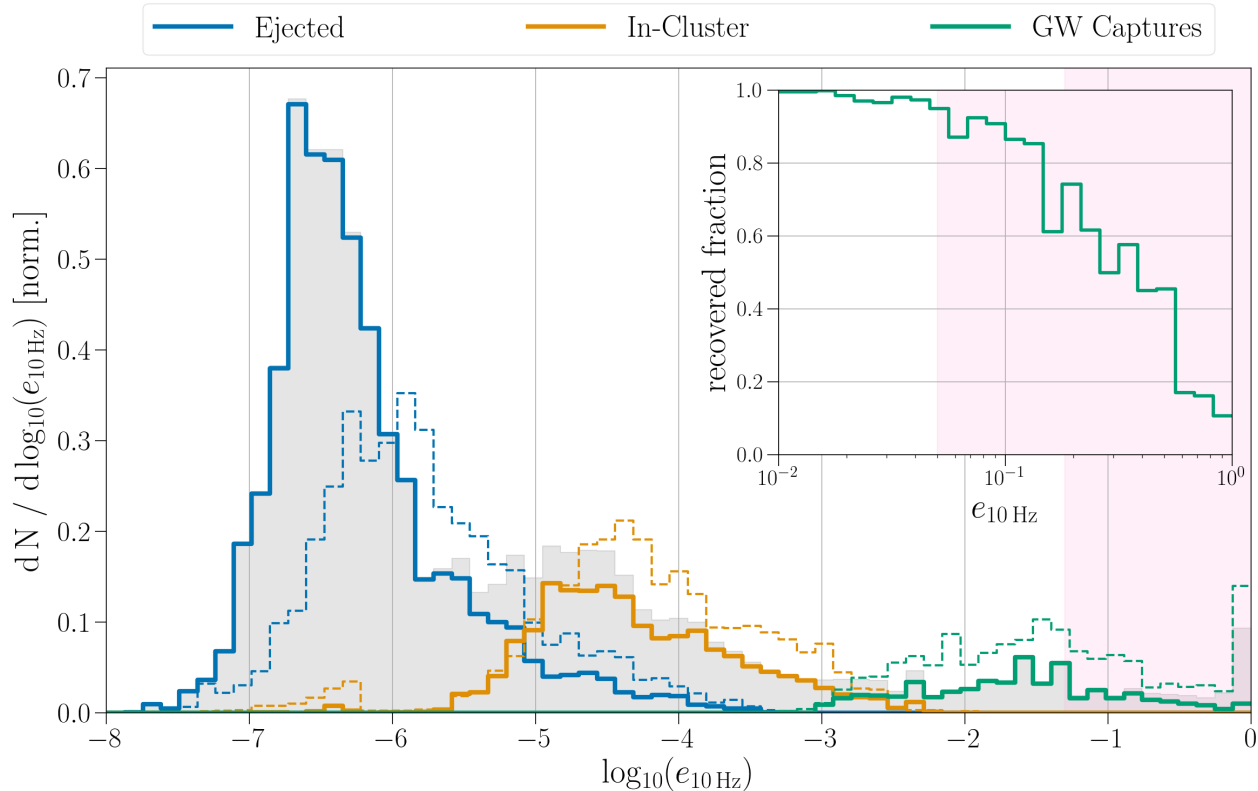


Figure 1. Eccentricity distributions for detectable BBH mergers assuming perfectly-matching templates (gray shade), circular templates (solid lines), and neglecting detection probabilities p_{det} altogether (dashed lines). Colored lines denote whether the BBH system was ejected from the cluster (blue), merged inside the cluster between strong dynamical interactions (orange), or merged as a capture during a strong gravitational encounter (green). The difference between the background gray histogram and solid-line histogram for the GW capture population shows the systems that are “missed” by searching with circular templates; this recovered fraction is also shown in the inset panel as a function of eccentricity. The detectable distribution assuming circular templates is normalized to the detectable distribution assuming perfectly-matching templates to better visualize this difference, and thus the solid line histograms integrate to slightly less than unity. The pink shaded region marks systems with $e_{10 \text{ Hz}} > 0.05$, the approximate eccentricity requirement for distinguishing GW150914-like systems from circular. Ejected mergers are more prevalent in the detectable distribution because more massive systems are ejected earlier in the history of the cluster and have longer inspiral timescales so that they can readily merge in the local universe.

In addition to the detection probability of eccentric sources, another important aspect of this analysis is determining the minimum eccentricity that is required for parameter estimation routines to be able to confidently distinguish a system as eccentric. For systems with properties similar to GW150914, Lower et al. (2018) found this threshold eccentricity to be $e_{\text{thresh}} \simeq 0.05$. This is consistent with the eccentricity upper-limits for GWTC-1 events from Romero-Shaw et al. (2019). Due to the computational expense of performing eccentric parameter estimation over a wide range of source parameters, we choose to adopt a threshold eccentricity of $e_{\text{thresh}} = 0.05$ for this analysis, where e_{thresh} is likewise defined at a reference GW frequency of 10 Hz. At this threshold, $\simeq 7\%$ of the potentially detectable distribution of cluster binaries have $e_{10 \text{ Hz}} > e_{\text{thresh}}$. We find

that reasonable variations in this parameter only lead to differences of order unity for our main results.

4. IMPLICATIONS OF ECCENTRIC DETECTIONS

Accounting for eccentricity in the selection effects afflicting the cluster population alters the detectable population. Under the assumption that matched-filter searches are the only means of detection (i.e., using circular templates for determining the detection probabilities as shown with the green line in Figure 2), we find a steep decrease in recovered systems for $e_{10 \text{ Hz}} \gtrsim 0.1$; see the inset of Figure 1. Using $e_{\text{thresh}} = 0.05$ as the characteristic threshold for systems that will be measurably eccentric, we find that only 56% of systems with $e_{10 \text{ Hz}} \geq e_{\text{thresh}}$ will be recovered using matched-filter searches. Thus, measurably eccentric systems from clusters make up $\simeq 4\%$ of the detectable distribution of

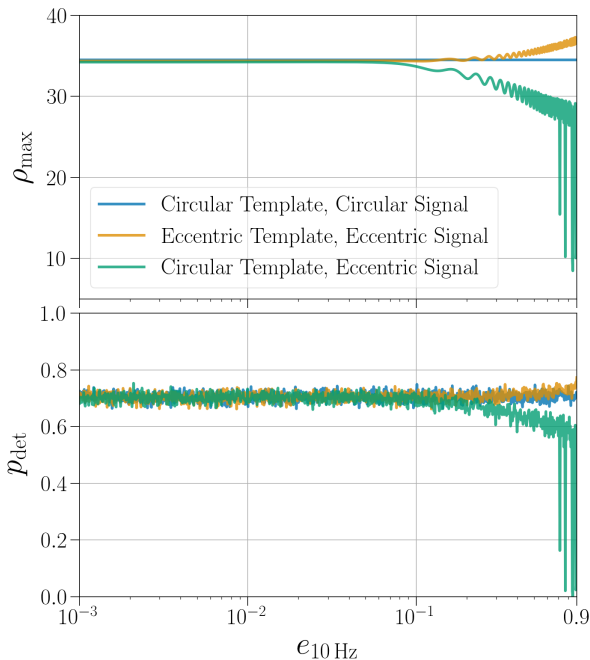


Figure 2. Time- and phase-maximized matched-filter SNR ρ_{\max} (*top panel*) and detection probability p_{det} (*bottom panel*) over a range of $e_{10\text{ Hz}}$. For this demonstration, we use a fiducial zero-spin system with mass $m_1 = 36M_{\odot}$ and $m_2 = 29M_{\odot}$, a luminosity distance $d_L = 1\text{ Gpc}$, and a midhighlatelow PSD (power spectral density) noise curve. The three colored curves represent the three signal–template combinations described in Section 3: a circular signal with a circular template (blue), an eccentric signal with an eccentric template (yellow), and an eccentric signal with a circular template (green). At high eccentricities ($e_{10\text{ Hz}} \gtrsim 0.1$) the time- and phase-maximized SNR slightly increases for the eccentric template/eccentric signal case since the template can perfectly match the amplitude and phase modulations caused by eccentricity in the inspiral. It decreases for the circular template/eccentric signal case because of the mismatch between the template and the eccentric signal.

BBH mergers from clusters. We refer to the fraction of measurably eccentric and detectable systems relative to the full detectable population as the detectable eccentric fraction ξ_{ecc} , which allows us to translate the presence or absence of eccentric detections to information about the fraction of mergers taking place in dense clusters. For the following analyses, we use our calculated value of $\xi_{\text{ecc}} = 3.9 \times 10^{-2}$.

Assuming dense star clusters account for a branching fraction β_c of the total number of observed BBH mergers and are the dominant contributor of eccentric sources, the probability of detecting N_{ecc} measurably eccentric

systems given N_{obs} total BBH detections follows a homogeneous Poisson process:

$$p(N_{\text{ecc}}|\lambda) = e^{-\lambda} \lambda^{N_{\text{ecc}}} / N_{\text{ecc}}!, \quad (1)$$

where

$$\lambda \equiv \xi_{\text{ecc}} \beta_c N_{\text{obs}}, \quad (2)$$

is the expected number of measurably eccentric detections after N_{obs} total observations. At a given N_{obs} and N_{ecc} , we can determine the likelihood for the cluster branching fraction β_c by evaluating a grid of β_c in the cumulative distribution function (CDF) of Eq. 1.

Constraints on β_c as a function of N_{obs} conditioned on various assumed measurably eccentric observations N_{ecc} are shown in Figure 3, with colored bands marking the symmetric 95% credible interval on β_c . We plot unphysical values of $\beta_c > 1$ as a means of a posterior predictive check; though clusters cannot account for *more* than the entire observed population of BBHs, significant support for β_c in this region at a given N_{obs} and N_{ecc} indicates issues in the underlying cluster models due to the observation of too many eccentric systems.

We first consider the implications of *not* detecting measurably eccentric BBH mergers on the cluster branching fraction. At the number of BBH observations through the first half of the third observing run (O3a), the non-detection of a bona fide eccentric signal does not yet place tension on clusters dominating the detectable rate of BBHs; $\beta_c = 1$ lies at the 83rd percentile of the likelihood. However, the non-detection of an eccentric signal will soon place interesting upper limits on the cluster branching fraction. At 100 (300) BBH observations, the lack of a bona fide eccentric signal will indicate $\beta_c < 0.77$ (0.26) at 95% credibility. Once $\simeq 150$ BBH observations have been made, the lack of a bona fide eccentric signal would indicate that clusters do not account for the majority of the detectable population ($\beta_c < 0.5$).

No unambiguous eccentric detections have been found in the GW catalogs to date. However, multiple studies have found marginal to strong evidence that GW190521, the most massive BBH system observed with GWs so far (Abbott et al. 2020b), is more consistent with being eccentric (Romero-Shaw et al. 2020; Gayathri et al. 2020) or from a hyperbolic encounter (Bustillo et al. 2021; Gamba et al. 2021) than a quasi-circular inspiral. Scattering experiments simulating the strong gravitational encounters typical of BHs in clusters indicate that GW190521-like binaries can enter the LIGO–Virgo band with appreciable eccentricity (though not at extreme eccentricities of $e_{10\text{ Hz}} \gtrsim 0.7$, see Holgado et al. 2021). A detailed analysis investigating eccentricity in

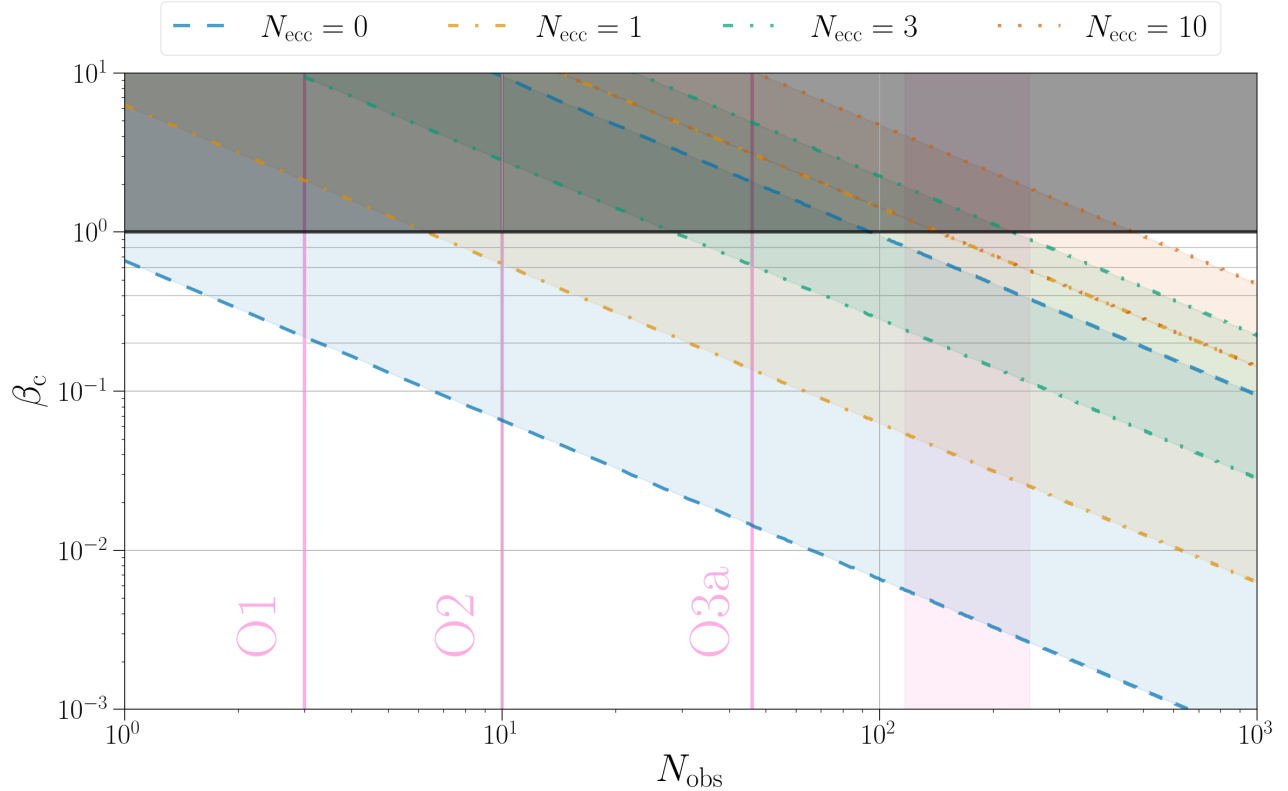


Figure 3. Constraints on the detectable branching fraction of the dense star cluster channel, β_c , as a function of number of BBH observations N_{obs} , under the condition of N_{ecc} eccentric observations. Colored bands encompass the 95% symmetric credible region of the β_c likelihood. We allow for branching fractions above the physical limit of $\beta_c = 1$ in our likelihood (black shaded region) to display combinations of N_{ecc} and N_{obs} that are unphysical, indicating issues with the underlying formation channel model. Pink vertical lines mark the number of confident BBH observations reported so far in the first (O1), second (O2), and first half of the third (O3a) observing runs by the LVC. The vertical pink shaded region marks the predicted number of BBH observations after the fourth observing run (O4) from Abbott et al. (2018), assuming the second half of the third observing run observes the same number of BBH systems as O3a.

the BBH mergers from the second GW catalog (GWTC-2; Abbott et al. 2020b) is in preparation.

Operating under the assumption that N_{ecc} out of the $N_{\text{obs}} = 46$ BBH observations in GWTC-2 are measurably eccentric, we now focus on the constraints that can be placed on β_c given the presence of eccentric observations. Figure 4 shows the likelihood for β_c assuming different values of N_{ecc} at $N_{\text{obs}} = 46$. Though the likelihood can have support at $\beta_c > 1$, we also mark the $> 5\%$ quantile of the posterior distribution with shaded regions, where we assume a flat-in-log prior with zero support above $\beta_c > 1$, thus constraining β_c to its physically valid range. Given one (two) eccentric signal(s) in GWTC-2, one can place a lower limit on the detectable branching fraction of BBHs originating from clusters of 0.14 (0.27) at the 95% credible level.

An important diagnostic for determining the fidelity of the cluster models considered in this work is identifying the number of eccentric observations that would be infeasible at a given N_{obs} . We quantify this by

the likelihood volume that satisfies $\beta_c \leq 1$, i.e. where there is non-zero prior probability. Given the number of BBH observations in GWTC-2, we find that there would be significant tension with eccentricity predictions from cluster models if $N_{\text{ecc}} \geq 4$, as $\gtrsim 96\%$ of the likelihood volume would be in the prior-excluded volume. Observing this many eccentric mergers in the current catalog of BBH observations may also be an indication that a formation channel other than dense stellar clusters is significantly contributing to the eccentric BBH population.

As N_{ecc} grows, tighter constraints on β_c are achieved since the width of the $\log_{10}(\beta_c)$ likelihood is independent of N_{obs} . At $N_{\text{ecc}} = 1$ (3), the symmetric 95% credible region for β_c is constrained to 1.36 (0.90) dex. Precision of ≈ 0.5 dex for the 95% credible range on β_c will be achieved at $N_{\text{ecc}} \gtrsim 10$.

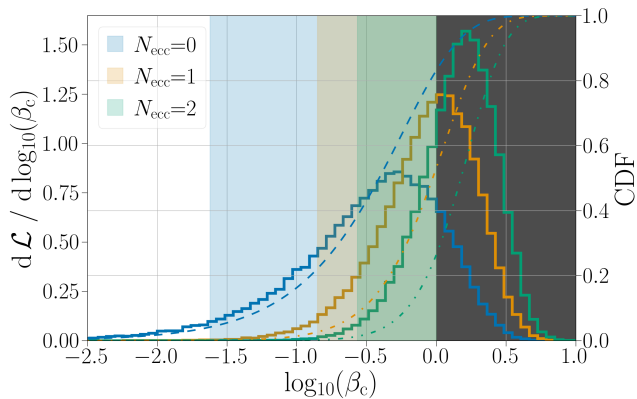


Figure 4. Constraints on the detectable branching fraction of the dense star cluster channel, β_c , conditioned on N_{ecc} eccentric observations of out $N_{\text{obs}} = 46$ total BBH observations. As with Figure 3, we show the likelihood without imposing the physical constraint of $\beta_c \leq 1$ with solid lines and the corresponding CDF with dashed lines; the unphysical region $\beta_c > 1$ is shaded in gray. Colored shaded regions mark the $> 5\%$ quantile of the *posterior* distribution, in which we impose a flat-in-log prior on β_c with no support for $\beta_c > 1$, and can be interpreted as *a posteriori* lower bounds on the cluster branching fraction given N_{ecc} eccentric observations. The relative location where the CDF crosses $\beta_c = 1$ corresponds to the evidence of models in which N_{ecc} eccentric BBH systems are observed given 46 total BBH observations.

5. DISCUSSION AND CONCLUSIONS

In this work, we show how the detection or non-detection of measurably eccentric GW sources can act to significantly constrain the contribution of certain dynamical channels to the detectable BBH population. Our main results are:

1. Dense star cluster models robustly predict that $\approx 7\%$ of potentially detectable sources will be measurably eccentric, though matched-filter searches will only recover $\approx 56\%$ of this cluster subpopulation.
2. Though the non-detection of a measurably eccentric source in GWTC-2 would not rule out the hypothesis that clusters are the dominant contributor of detectable sources, once 150 BBH observations have been made, the lack of a bona fide eccentric observation would indicate that clusters do not make up more than 50% of the detectable population of BBHs. Even with pessimistic predictions, this number of BBH mergers will be reached in O4.
3. Assuming that it originated in a dense star cluster, a single measurably eccentric source in GWTC-2 would indicate that such clusters account for $> 14\%$ of the detectable BBH population.

4. Once 10 eccentric observations from clusters have been made, the detectable branching fraction from clusters will be constrained at the 0.5-dex level.

Eccentricity may be the most robust indicator of a dynamical BBH formation pathway, as the presence of eccentric mergers in clusters is relatively insensitive to uncertain physical processes that impact other dynamical indicators, such as binary evolution physics, the efficiency of angular momentum transport in massive stars, and the location of the pair instability mass gap. Instead, eccentric mergers in dynamical environments are the result of well-understood physics, and if BHs are indeed present in clusters, eccentric mergers are an inevitable byproduct.

Current state-of-the-art models of dense star clusters predict local BBH merger rates of $\sim 2 - 20 \text{ Gpc}^{-3} \text{ yr}^{-1}$ (Kremer et al. 2020; Rodriguez et al. 2021). Based on this work, this would translate to a merger rate of measurably eccentric sources of $\sim 0.08 - 0.8 \text{ Gpc}^{-3} \text{ yr}^{-1}$. The merger rate from dense star clusters is comparable to the empirically-measured rate by the LVC following GWTC-2 of $15 - 39 \text{ Gpc}^{-3} \text{ yr}^{-1}$ (90% credibility, Abbott et al. 2020a). However, it is likely that globular clusters only account for a portion of this rate, and the diversity of BBH observations to date hint at multiple formation channels significantly contributing to the observed population of BBHs (Abbott et al. 2020a; Zevin et al. 2021). Eccentric sources are useful for constraining the merger rate from clusters, thereby constraining the rate contribution of other formation channels.

This analysis estimates eccentric detectability assuming only matched-filter searches with circular, aligned-spin templates. Though these searches are the main workhorse for the detection of compact binary coalescences, a number of other search techniques are used to identify GW signals. Of particular pertinence to this study are burst searches, which are unmodeled searches that identify coincident and coherent signals in the GW data stream. For nearby and loud mergers, burst searches would excel over quasi-circular template-based searches at detecting highly-eccentric systems (Klimenko et al. 2016). A possible example of this in action is GW190521, which was found by a burst search to have a much lower false-alarm rate (< 1 per 28 years) than reported for the same candidate by matched-filter compact binary pipelines (≥ 1 per 8 years) (Abbott et al. 2020c). In addition, higher matched-filter SNRs may be achieved by marginalizing over intrinsic parameters of the template rather than considering a single circular template with analogous source properties. Thus, the detectable eccentric fraction ξ_{ecc} we report can be

considered a lower limit. However, if one were to assume the limiting case where eccentric mergers are equally as likely to be detected than their circular counterparts, the maximum detectable eccentric fraction is less than twice our reported value. Therefore, even in this best-case detectability scenario, our constraints on branching fractions as a function of the number of BBH observations are reduced by less than a factor of two.

We also assume that strong gravitational encounters in clusters are the only means of generating measurably eccentric mergers in the LIGO–Virgo sensitive frequency range. Other formation channels, such as the secular evolution of isolated hierarchical systems (Antognini et al. 2014; Silsbee & Tremaine 2017; Antonini et al. 2017; Rodriguez & Antonini 2018; Liu & Lai 2019; Fragione & Kocsis 2019), BBH systems orbiting a supermassive BH in galactic nuclei (O’Leary et al. 2009; Antonini & Perets 2012; Petrovich & Antonini 2017; Hoang et al. 2018; Stephan et al. 2019; Takatsy et al. 2019; Fragione et al. 2019a,b), and active galactic nuclei disks (Gröbner et al. 2020; Samsing et al. 2020b; Tagawa et al. 2021) have all been proposed for generating systems with measurable eccentricities. Though the predicted local merger rates and eccentricity distributions for these channels are more uncertain, if these channels contribute significantly to the measurably eccentric merger rate they would impact the branching fraction constraints reported in this work. Robust rate estimates and eccentricity distributions from these channels could be incorporated into the methodology presented here, allowing for mixture models to be created with multiple eccentric detection efficiencies and joint constraints on the contribution of formation channels that generate eccentric BBH mergers.

The utility of eccentric detections for constraining formation channels will improve as more BBH mergers are observed, regardless of whether or not eccentric mergers are observed in this population. The eccentric detection efficiency will also be relatively stable as the sensitivity of the detector network improves, as the fraction of measurably eccentric mergers relative to the full cluster population does not evolve significantly with redshift (Rodriguez et al. 2018a). Given current BBH rate measurements and the anticipated sensitivity of the GW detector network in O4, the lack of a measurably eccentric detection after O4 will indicate that clusters do not account for the majority of BBH mergers. On the other hand, with future eccentric detections we would significantly constrain the lower limit of mergers that result from clusters and other dynamical channels. Once ~ 10 eccentric BBH mergers are observed, constraints on the dynamical branching fraction

will reach the 0.5-dex level, potentially making eccentricity the most robust and efficient means for constraining formation pathways of BBH mergers.

ACKNOWLEDGMENTS

We thank Rossella Gamba for useful comments on this manuscript, Carl Rodriguez for assistance computing the relative weights for the CMC cluster models, Daniel Holz for enlightening discussions, and Alessandro Nagar, Sebastiano Bernuzzi, and Piero Rettengo for help with and development of the TEOBResumS waveform model. Support for this work and for M.Z. was provided by NASA through the NASA Hubble Fellowship grant HST-HF2-51474.001-A awarded by the Space Telescope Science Institute, which is operated by the Association of Universities for Research in Astronomy, Inc., for NASA, under contract NAS5-26555. K.K. is supported by an NSF Astronomy and Astrophysics Postdoctoral Fellowship under award AST-2001751. E.T. and P.D.L. are supported through Australian Research Council (ARC) Centre of Excellence CE170100004. P.D.L. is supported through ARC Future Fellowship FT160100112, and ARC Discovery project DP180103155. This work used computing resources at CIERA funded by NSF grant No. PHY-1726951 and resources and staff provided by the Quest high-performance computing facility at Northwestern University, which is jointly supported by the Office of the Provost, the Office for Research, and Northwestern University Information Technology.

Software: Astropy (Robitaille et al. 2013; Price-Whelan et al. 2018); iPython (Pérez & Granger 2007); Matplotlib (Hunter 2007); NumPy (Oliphant 2006; Van Der Walt et al. 2011); Pandas (McKinney 2010); PyCBC (Nitz et al. 2019); SciPy (Virtanen et al. 2020); TEOBResumS (Nagar et al. 2018).

APPENDIX

A. CLUSTER MODELS AND ECCENTRICITY OF BBH SOURCES

In each cluster model, the component masses, component spin magnitudes, and merger redshifts of BBH mergers are recorded. BHs are assumed to have negligible birth spin, as predicted if angular momentum transport in their massive-star progenitors is highly efficient (Spruit 1999, 2002; Fuller et al. 2019), though spin can be imparted in cluster BHs through prior BBH merger events that are retained in the cluster. Spin tilts are assumed to be isotropically distributed on the sphere. BBHs in our models have (source-frame) total masses between 14–135 M_{\odot} , mass ratios between 0.3–1.0, and effective spins between -0.42 – 0.42 , where the quoted ranges represent 99% of all systems. Following the approach in Rodriguez & Loeb (2018) and Martinez et al. (2021), each cluster model also is assigned a relative astrophysical weight, γ_c , based on the cluster model’s mass and metallicity.

The orbital integration of merging BBHs is halted once the component BHs reach a separation of 10 M, and the semi-major axis and eccentricity of the orbit are recorded at various discrete separations prior to this point (see Rodriguez et al. 2018a for further discussion on halting criteria). To acquire the orbital properties at a particular GW frequency f_{GW} for a binary of total mass M_{tot} , we use the orbital properties recorded at a separation of 100 M and numerically solve for the orbital properties at an eccentric peak frequency as in Wen (2003):

$$a(e) = \frac{1}{1 - e^2} \left[\frac{GM_{\text{tot}} (1 + e)^{1.1954}}{\pi f_{\text{GW}}} \right]^{2/3}, \quad (\text{A1})$$

which is coupled to the differential equation governing the coevolution of semi-major axis and eccentricity from Peters (1964):

$$\left\langle \frac{da}{de} \right\rangle = \frac{12 a}{19 e} \frac{[1 + (73/24)e^2 + (37/96)e^4]}{(1 - e^2)[1 + (121/304)e^2]}. \quad (\text{A2})$$

In certain cases, the binary forms through a hyperbolic capture at frequencies above f_{GW} , and we assign its eccentricity at f_{GW} to an extremal value of $e_{\text{max}} = 0.9$.

As we are interested in the properties of detectable BBH mergers rather than the underlying population, we must also account for the larger amount of comoving volume accessible at higher redshifts and the relative sensitivity of GW detectors to BBHs with different properties. Each system i , parameterized by component masses m_1 and m_2 , component spin vectors χ_1 and χ_2 , merger redshift z , eccentricity at a reference frequency of 10 Hz $e_{10 \text{ Hz}}$, and cluster weight γ_c is given a normalized detectability weight of

$$w_i = \left[\gamma_c \frac{dV_c}{dz} \frac{dt_s}{dt_0} p_{\text{det}}(m_1, m_2, \chi_1, \chi_2, e_{10 \text{ Hz}}, z) \right]_i \quad (\text{A3})$$

where $\frac{dV_c}{dz}$ is the comoving volume element at redshift z , $\frac{dt_s}{dt_0} = (1 + z)^{-1}$ is the time dilation between clocks at the merger redshift and on Earth, and p_{det} is the detection probability of a system with a given set of intrinsic parameters, defined in the following section.

B. DETECTABILITY OF ECCENTRIC SOURCES

We estimate detection probabilities using a fixed SNR threshold required for detection of $\rho_{\text{thresh}} = 8.0$. Given the source parameters of each system, we calculate a matched-filter SNR assuming the optimal orientation of face-on and directly overhead:

$$\rho_{\text{max}}^2 = \frac{1}{\langle h|h \rangle} | \langle s|h \rangle |^2 \quad (\text{B4})$$

where we maximize over phase and time of coalescence, and $\langle s|h \rangle$ is the noise-weighted inner product:

$$\langle s|h \rangle = 4 \int_0^{\infty} \frac{\tilde{s}(f) \tilde{h}^*(f)}{S_n(f)} df \quad (\text{B5})$$

with $\tilde{s}(f)$ and $\tilde{h}(f)$ being the Fourier transform of the time-domain signal and template, respectively, and $S_n(f)$ the one-sided average PSD of the detector noise. The noise-weighted inner product of the template with itself $\langle h|h \rangle$

is the optimal matched-filter SNR and defined similarly. We assume a stationary, single-detector LIGO PSD with `midhighlatelow` sensitivity from Abbott et al. (2018), which has been shown to be a decent approximation to the more sophisticated approach of injection/recovery campaigns in search pipelines (e.g., Abbott et al. 2018; Nitz et al. 2020).

For the three matched-filter cases described in Section 3, we window the waveforms with a Tukey filter, and in cases where the signal and template are not identical, we zero-pad the shorter waveform, time-align the maximum strain of the template and signal, and apply a frequency-domain time- and phase-shift determined by maximizing the overlap integral. If $\rho_{\max} < \rho_{\text{thresh}}$, detection probabilities are assigned to be zero. Otherwise, we determine detection probabilities by Monte Carlo sampling uniformly over the extrinsic parameters ψ and multiplying the maximized SNR with the detector projection factor $\Theta(\psi) \in [0, 1]$ (Finn & Chernoff 1993). The detection probability is thus determined as

$$p_{\text{det}} = \sum_{j=1}^N \mathcal{H}[\Theta(\psi_j)\rho_{\max} - \rho_{\text{thresh}}] \quad (\text{B6})$$

where \mathcal{H} is the Heaviside step function, and we draw $N = 10^3$ sets of extrinsic parameters.

REFERENCES

- Aasi, J., Abbott, B. P., Abbott, R., et al. 2015, *Classical and Quantum Gravity*, 32, 074001, doi: [10.1088/0264-9381/32/7/074001](https://doi.org/10.1088/0264-9381/32/7/074001)
- Abbott, B. P., Abbott, R., Abbott, T. D., et al. 2016, *Physical Review Letters*, 116, 1, doi: [10.1103/PhysRevLett.116.061102](https://doi.org/10.1103/PhysRevLett.116.061102)
- . 2018, *Living Reviews in Relativity*, 21, 57, doi: [10.1007/s41114-018-0012-9](https://doi.org/10.1007/s41114-018-0012-9)
- . 2019a, *The Astrophysical Journal*, 883, 149, doi: [10.3847/1538-4357/ab3c2d](https://doi.org/10.3847/1538-4357/ab3c2d)
- . 2019b, *Physical Review X*, 9, 31040, doi: [10.1103/PhysRevX.9.031040](https://doi.org/10.1103/PhysRevX.9.031040)
- Abbott, R., Abbott, T. D., Abraham, S., et al. 2020a, arXiv e-prints. <https://arxiv.org/abs/2010.14533>
- . 2020b, arXiv e-prints. <https://arxiv.org/abs/2010.14527>
- . 2020c, *Physical Review Letters*, 125, 101102, doi: [10.1103/PhysRevLett.125.101102](https://doi.org/10.1103/PhysRevLett.125.101102)
- Acernese, F., Agathos, M., Agatsuma, K., et al. 2015, *Classical and Quantum Gravity*, 32, 024001, doi: [10.1088/0264-9381/32/2/024001](https://doi.org/10.1088/0264-9381/32/2/024001)
- Adams, T., Buskulis, D., Germain, V., et al. 2016, *Classical and Quantum Gravity*, 33, doi: [10.1088/0264-9381/33/17/175012](https://doi.org/10.1088/0264-9381/33/17/175012)
- Ade, P. A., Aghanim, N., Arnaud, M., et al. 2016, *Astronomy and Astrophysics*, 594, A13, doi: [10.1051/0004-6361/201525830](https://doi.org/10.1051/0004-6361/201525830)
- Albanesi, S., Nagar, A., & Bernuzzi, S. 2021, arXiv e-prints. <https://arxiv.org/abs/2104.10559>
- Allen, B., Anderson, W. G., Brady, P. R., Brown, D. A., & Creighton, J. D. 2012, *Physical Review D - Particles, Fields, Gravitation and Cosmology*, 85, 1, doi: [10.1103/PhysRevD.85.122006](https://doi.org/10.1103/PhysRevD.85.122006)
- Antognini, J. M., Shappee, B. J., Thompson, T. A., & Amaro-seoane, P. 2014, *Monthly Notices of the Royal Astronomical Society*, 439, 1079, doi: [10.1093/mnras/stu039](https://doi.org/10.1093/mnras/stu039)
- Antonini, F., & Gieles, M. 2020, *Physical Review D*, 102, 123016, doi: [10.1103/PhysRevD.102.123016](https://doi.org/10.1103/PhysRevD.102.123016)
- Antonini, F., & Perets, H. B. 2012, *The Astrophysical Journal*, 757, 27, doi: [10.1088/0004-637X/757/1/27](https://doi.org/10.1088/0004-637X/757/1/27)
- Antonini, F., Toonen, S., & Hamers, A. S. 2017, *The Astrophysical Journal*, 841, 77, doi: [10.3847/1538-4357/aa6f5e](https://doi.org/10.3847/1538-4357/aa6f5e)
- Arca Sedda, M., Askar, A., & Giersz, M. 2018, *Monthly Notices of the Royal Astronomical Society*, 479, 4652, doi: [10.1093/mnras/sty1859](https://doi.org/10.1093/mnras/sty1859)
- Aubin, F., Brighenti, F., Chierici, R., et al. 2021, arXiv e-prints, doi: [10.1088/1361-6382/abe913](https://doi.org/10.1088/1361-6382/abe913)
- Banerjee, S. 2017, *Monthly Notices of the Royal Astronomical Society*, 467, 524, doi: [10.1093/mnras/stx2347](https://doi.org/10.1093/mnras/stx2347)
- Bartos, I., Kocsis, B., Haiman, Z., & Márka, S. 2017, *The Astrophysical Journal*, 835, 165, doi: [10.3847/1538-4357/835/2/165](https://doi.org/10.3847/1538-4357/835/2/165)
- Bavera, S. S., Fragos, T., Zevin, M., et al. 2021, *Astronomy and Astrophysics*, 647, A153, doi: [10.1051/0004-6361/202039804](https://doi.org/10.1051/0004-6361/202039804)
- Belczynski, K., Holz, D. E., Bulik, T., & O’shaughnessy, R. 2016, *Nature*, 534, 512, doi: [10.1038/nature18322](https://doi.org/10.1038/nature18322)
- Bethe, H. A., & Brown, G. E. 1998, *The Astrophysical Journal*, 506, 780, doi: [10.1086/306265](https://doi.org/10.1086/306265)
- Bird, S., Cholis, I., Muñoz, J. B., et al. 2016, *Physical Review Letters*, 116, 1, doi: [10.1103/PhysRevLett.116.201301](https://doi.org/10.1103/PhysRevLett.116.201301)

- Bouffanais, Y., Mapelli, M., Santoliquido, F., et al. 2021, arXiv e-prints.
<https://arxiv.org/abs/arXiv:2102.12495v1>
- Breen, P. G., & Heggie, D. C. 2013, *Monthly Notices of the Royal Astronomical Society*, 436, 584,
 doi: [10.1093/mnras/stt1599](https://doi.org/10.1093/mnras/stt1599)
- Buonanno, A., & Damour, T. 1999, *Physical Review D*, 59, 084006
- . 2000, *Physical Review D*, 62, 064015,
 doi: [10.1103/PhysRevD.62.064015](https://doi.org/10.1103/PhysRevD.62.064015)
- Bustillo, J. C., Sanchis-Gual, N., Torres-Forné, A., et al. 2021, *Physical Review Letters*, 126, 1,
 doi: [10.1103/PhysRevLett.126.081101](https://doi.org/10.1103/PhysRevLett.126.081101)
- Chatterjee, S., Rodriguez, C. L., Kalogera, V., & Rasio, F. A. 2017, *The Astrophysical Journal*, 836, L26,
 doi: [10.3847/2041-8213/aa5caa](https://doi.org/10.3847/2041-8213/aa5caa)
- Chiaromello, D., & Nagar, A. 2020, *Physical Review D*, 101, 101501, doi: [10.1103/PhysRevD.101.101501](https://doi.org/10.1103/PhysRevD.101.101501)
- Chu, Q., Kovalam, M., Wen, L., et al. 2020, arXiv e-prints.
<https://arxiv.org/abs/2011.06787>
- Clesse, S., & Garcia-Bellido, J. 2020, arXiv e-prints.
<https://arxiv.org/abs/2007.06481>
- Dal Canton, T., Nitz, A. H., Lundgren, A. P., et al. 2014, *Physical Review D - Particles, Fields, Gravitation and Cosmology*, 90, 1, doi: [10.1103/PhysRevD.90.082004](https://doi.org/10.1103/PhysRevD.90.082004)
- Damour, T. 2001, *Physical Review D*, 64, 124013,
 doi: [10.1103/PhysRevD.64.124013](https://doi.org/10.1103/PhysRevD.64.124013)
- Damour, T., Jaranowski, P., & Schäfer, G. 2000, *Physical Review D*, 62, 084011, doi: [10.1103/PhysRevD.62.084011](https://doi.org/10.1103/PhysRevD.62.084011)
- . 2015, *Physical Review D*, 91, 084024,
 doi: [10.1103/PhysRevD.91.084024](https://doi.org/10.1103/PhysRevD.91.084024)
- Damour, T., & Nagar, A. 2014, *Physical Review D*, 90, 044018, doi: [10.1103/PhysRevD.90.044018](https://doi.org/10.1103/PhysRevD.90.044018)
- Davies, G. S., Dent, T., Tápai, M., et al. 2020, *Physical Review D*, 102, 22004,
 doi: [10.1103/PhysRevD.102.022004](https://doi.org/10.1103/PhysRevD.102.022004)
- Di Carlo, U. N., Giacobbo, N., Mapelli, M., et al. 2019, *Monthly Notices of the Royal Astronomical Society*, 487, 2947, doi: [10.1093/mnras/stz1453](https://doi.org/10.1093/mnras/stz1453)
- Dominik, M., Belczynski, K., Fryer, C., et al. 2012, *The Astrophysical Journal*, 759, 52,
 doi: [10.1088/0004-637X/759/1/52](https://doi.org/10.1088/0004-637X/759/1/52)
- Downing, J. M. B., Benacquista, M. J., Giersz, M., & Spurzem, R. 2010, *Monthly Notices of the Royal Astronomical Society*, 407, 1946,
 doi: [10.1111/j.1365-2966.2010.17040.x](https://doi.org/10.1111/j.1365-2966.2010.17040.x)
- Finn, L. S., & Chernoff, D. F. 1993, *Physical Review D*, 47, 2198, doi: [10.1103/PhysRevD.47.2198](https://doi.org/10.1103/PhysRevD.47.2198)
- Fragione, G., & Bromberg, O. 2019, *Monthly Notices of the Royal Astronomical Society*, 488, 4370,
 doi: [10.1093/mnras/stz2024](https://doi.org/10.1093/mnras/stz2024)
- Fragione, G., Grishin, E., Leigh, N. W. C., Perets, H. B., & Perna, R. 2019a, *Monthly Notices of the Royal Astronomical Society*, 488, 2825,
 doi: [10.1093/mnras/stz1803](https://doi.org/10.1093/mnras/stz1803)
- Fragione, G., & Kocsis, B. 2018, *Physical Review Letters*, 121, 161103, doi: [10.1103/PhysRevLett.121.161103](https://doi.org/10.1103/PhysRevLett.121.161103)
- . 2019, *Monthly Notices of the Royal Astronomical Society*, 486, 4781, doi: [10.1093/mnras/stz1175](https://doi.org/10.1093/mnras/stz1175)
- Fragione, G., Leigh, N. W., & Perna, R. 2019b, *Monthly Notices of the Royal Astronomical Society*, 488, 2825,
 doi: [10.1093/mnras/stz1803](https://doi.org/10.1093/mnras/stz1803)
- Franciolini, G., Baibhav, V., De Luca, V., et al. 2021, arXiv e-prints. <https://arxiv.org/abs/2105.03349>
- Fregeau, J. M., Cheung, P., Zwart, S. F. P., & Rasio, F. A. 2004, *Monthly Notices of the Royal Astronomical Society*, 352, 1, doi: [10.1111/j.1365-2966.2004.07914.x](https://doi.org/10.1111/j.1365-2966.2004.07914.x)
- Fregeau, J. M., & Rasio, F. A. 2007, *The Astrophysical Journal*, 658, 1047, doi: [10.1086/511809](https://doi.org/10.1086/511809)
- Fuller, J., Piro, A. L., & Jermyn, A. S. 2019, *Monthly Notices of the Royal Astronomical Society*, 485, 3661,
 doi: [10.1093/mnras/stz514](https://doi.org/10.1093/mnras/stz514)
- Gamba, R., Breschi, M., Carullo, G., et al. 2021, arXiv e-prints. <https://arxiv.org/abs/2106.05575>
- Gayathri, V., Healy, J., Lange, J., et al. 2020, arXiv e-prints. <https://arxiv.org/abs/2009.05461>
- Giesers, B., Dreizler, S., Husser, T. O., et al. 2018, *Monthly Notices of the Royal Astronomical Society: Letters*, 475, L15, doi: [10.1093/mnrasl/slx203](https://doi.org/10.1093/mnrasl/slx203)
- Giesers, B., Kamann, S., Dreizler, S., et al. 2019, *Astronomy and Astrophysics*, 632,
 doi: [10.1051/0004-6361/201936203](https://doi.org/10.1051/0004-6361/201936203)
- Gondán, L., & Kocsis, B. 2020, arXiv e-prints.
<https://arxiv.org/abs/arXiv:2011.02507v1>
- Gröbner, M., Ishibashi, W., Tiwari, S., et al. 2020, *Astronomy and Astrophysics*, 638, 1,
 doi: [10.1051/0004-6361/202037681](https://doi.org/10.1051/0004-6361/202037681)
- Hoang, B.-M., Naoz, S., Kocsis, B., Rasio, F. A., & Dosopoulou, F. 2018, *The Astrophysical Journal*, 856, 140, doi: [10.3847/1538-4357/aaafce](https://doi.org/10.3847/1538-4357/aaafce)
- Holgado, A. M., Ortega, A., & Rodriguez, C. L. 2021, *The Astrophysical Journal Letters*, 909, L24,
 doi: [10.3847/2041-8213/abe7f5](https://doi.org/10.3847/2041-8213/abe7f5)
- Hooper, S., Chung, S. K., Luan, J., et al. 2012, *Physical Review D - Particles, Fields, Gravitation and Cosmology*, 86, 1, doi: [10.1103/PhysRevD.86.024012](https://doi.org/10.1103/PhysRevD.86.024012)
- Hunter, J. D. 2007, *Computing in Science and Engineering*, 9, 99, doi: [10.1109/MCSE.2007.55](https://doi.org/10.1109/MCSE.2007.55)

- Klimenko, S., Vedovato, G., Drago, M., et al. 2016, *Physical Review D*, 93, 1, doi: [10.1103/PhysRevD.93.042004](https://doi.org/10.1103/PhysRevD.93.042004)
- Kocsis, B., & Levin, J. 2012, *Physical Review D*, 85, 1, doi: [10.1103/PhysRevD.85.123005](https://doi.org/10.1103/PhysRevD.85.123005)
- Kremer, K., Chatterjee, S., Ye, C. S., Rodriguez, C. L., & Rasio, F. A. 2019, *The Astrophysical Journal*, 871, 38, doi: [10.3847/1538-4357/aaf646](https://doi.org/10.3847/1538-4357/aaf646)
- Kremer, K., Ye, C. S., Chatterjee, S., Rodriguez, C. L., & Rasio, F. A. 2018, *The Astrophysical Journal Letters*, 855, L15, doi: [10.3847/2041-8213/aab26c](https://doi.org/10.3847/2041-8213/aab26c)
- Kremer, K., Ye, C. S., Rui, N. Z., et al. 2020, *The Astrophysical Journal Supplement Series*, 247, 48, doi: [10.3847/1538-4365/ab7919](https://doi.org/10.3847/1538-4365/ab7919)
- Liu, B., & Lai, D. 2019, *Monthly Notices of the Royal Astronomical Society*, 483, 4060, doi: [10.1093/mnras/sty3432](https://doi.org/10.1093/mnras/sty3432)
- Loutrel, N. 2020, arXiv e-prints. <https://arxiv.org/abs/2009.11332>
- Lower, M. E., Thrane, E., Lasky, P. D., & Smith, R. 2018, *Physical Review D*, 98, 083028, doi: [10.1103/PhysRevD.98.083028](https://doi.org/10.1103/PhysRevD.98.083028)
- Mackey, A. D., Wilkinson, M. I., Davies, M. B., & Gilmore, G. F. 2007, *Monthly Notices of the Royal Astronomical Society: Letters*, 379, 40, doi: [10.1111/j.1745-3933.2007.00330.x](https://doi.org/10.1111/j.1745-3933.2007.00330.x)
- Martinez, M. A. S., Rodriguez, C. L., & Fragione, G. 2021, arXiv e-prints. <https://arxiv.org/abs/2105.01671>
- McKernan, B., Ford, K. E., Kocsis, B., Lyra, W., & Winter, L. M. 2014, *Monthly Notices of the Royal Astronomical Society*, 441, 900, doi: [10.1093/mnras/stu553](https://doi.org/10.1093/mnras/stu553)
- McKinney, W. 2010, in *Proceedings of the 9th Python in Science Conference*, ed. S. van der Walt & J. Millman, 51–56, doi: [10.25080/Majora-92bf1922-00a](https://doi.org/10.25080/Majora-92bf1922-00a)
- Messick, C., Blackburn, K., Brady, P., et al. 2017, *Physical Review D*, 95, 1, doi: [10.1103/PhysRevD.95.042001](https://doi.org/10.1103/PhysRevD.95.042001)
- Nagar, A., Bonino, A., & Rettegno, P. 2021, *Physical Review D*, 103, 104021, doi: [10.1103/physrevd.103.104021](https://doi.org/10.1103/physrevd.103.104021)
- Nagar, A., Bernuzzi, S., Del Pozzo, W., et al. 2018, *Physical Review D*, 98, 1, doi: [10.1103/PhysRevD.98.104052](https://doi.org/10.1103/PhysRevD.98.104052)
- Nitz, A., Harry, I., Brown, D., et al. 2019, *gwastro/pycbc: PyCBC Release v1.14.4*, Zenodo, doi: [10.5281/zenodo.3546372](https://doi.org/10.5281/zenodo.3546372)
- Nitz, A. H., Dent, T., Dal Canton, T., Fairhurst, S., & Brown, D. A. 2017, *The Astrophysical Journal*, 849, 118, doi: [10.3847/1538-4357/aa8f50](https://doi.org/10.3847/1538-4357/aa8f50)
- Nitz, A. H., Schäfer, M., & Canton, T. D. 2020, *The Astrophysical Journal Letters*, 902, L29, doi: [10.3847/2041-8213/abbc10](https://doi.org/10.3847/2041-8213/abbc10)
- O’Leary, R. M., Kocsis, B., & Loeb, A. 2009, *Monthly Notices of the Royal Astronomical Society*, 395, 2127, doi: [10.1111/j.1365-2966.2009.14653.x](https://doi.org/10.1111/j.1365-2966.2009.14653.x)
- O’Leary, R. M., Rasio, F. A., Fregeau, J. M., Ivanova, N., & O’Shaughnessy, R. 2006, *The Astrophysical Journal*, 637, 937, doi: [10.1086/498446](https://doi.org/10.1086/498446)
- Oliphant, T. E. 2006, *A guide to NumPy (USA: Trelgol Publishing)*. <https://web.mit.edu/dvp/Public/numpybook.pdf>
- Pérez, F., & Granger, B. E. 2007, *IEEE Journals & Magazines*, 9, 21, doi: [10.1109/MCSE.2007.53](https://doi.org/10.1109/MCSE.2007.53)
- Peters, P. C. 1964, *Physical Review*, 136, 1224, doi: [10.1103/PhysRev.136.B1224](https://doi.org/10.1103/PhysRev.136.B1224)
- Petrovich, C., & Antonini, F. 2017, *The Astrophysical Journal*, 846, 146, doi: [10.3847/1538-4357/aa8628](https://doi.org/10.3847/1538-4357/aa8628)
- Portegies Zwart, S. F., & McMillan, S. L. W. 2000, *The Astrophysical Journal Letters*, 528, 17, doi: [10.1086/312422](https://doi.org/10.1086/312422)
- Price-Whelan, A. M., Sipocz, B. M., Günther, H. M., et al. 2018, *The Astronomical Journal*, 156, 123, doi: [10.3847/1538-3881/aabc4f](https://doi.org/10.3847/1538-3881/aabc4f)
- Ramos-Buades, A., Tiwari, S., Haney, M., & Husa, S. 2020, *Physical Review D*, 102, 43005, doi: [10.1103/PhysRevD.102.043005](https://doi.org/10.1103/PhysRevD.102.043005)
- Robitaille, T. P., Tollerud, E. J., Greenfield, P., et al. 2013, *Astronomy & Astrophysics*, 558, A33, doi: [10.1051/0004-6361/201322068](https://doi.org/10.1051/0004-6361/201322068)
- Rodriguez, C. L., Amaro-seoane, P., Chatterjee, S., et al. 2018a, *Physical Review D*, 98, 123005, doi: [10.1103/PhysRevD.98.123005](https://doi.org/10.1103/PhysRevD.98.123005)
- Rodriguez, C. L., Amaro-Seoane, P., Chatterjee, S., & Rasio, F. A. 2018b, *Physical Review Letters*, 120, 151101, doi: [10.1103/PhysRevLett.120.151101](https://doi.org/10.1103/PhysRevLett.120.151101)
- Rodriguez, C. L., & Antonini, F. 2018, *The Astrophysical Journal*, 863, 7, doi: [10.3847/1538-4357/aacea4](https://doi.org/10.3847/1538-4357/aacea4)
- Rodriguez, C. L., Chatterjee, S., & Rasio, F. A. 2016, *Physical Review D*, 93, 084029, doi: [10.1103/PhysRevD.93.084029](https://doi.org/10.1103/PhysRevD.93.084029)
- Rodriguez, C. L., Kremer, K., Chatterjee, S., et al. 2021, *Research Notes of the AAS*, 5, 19, doi: [10.3847/2515-5172/abdf54](https://doi.org/10.3847/2515-5172/abdf54)
- Rodriguez, C. L., & Loeb, A. 2018, *The Astrophysical Journal Letters*, 866, L5, doi: [10.3847/2041-8213/aae377](https://doi.org/10.3847/2041-8213/aae377)
- Romero-Shaw, I., Lasky, P. D., Thrane, E., & Bustillo, J. C. 2020, GW190521: Orbital eccentricity and signatures of dynamical formation in a binary black hole merger signal, IOP Publishing, doi: [10.3847/2041-8213/abbe26](https://doi.org/10.3847/2041-8213/abbe26)
- Romero-Shaw, I. M., Lasky, P. D., & Thrane, E. 2019, *Monthly Notices of the Royal Astronomical Society*, 490, 5210, doi: [10.1093/mnras/stz2996](https://doi.org/10.1093/mnras/stz2996)

- Samsing, J. 2018, *Physical Review D*, 97, 103014, doi: [10.1103/PhysRevD.97.103014](https://doi.org/10.1103/PhysRevD.97.103014)
- Samsing, J., Askar, A., & Giersz, M. 2018, *The Astrophysical Journal*, 855, 124, doi: [10.3847/1538-4357/aaab52](https://doi.org/10.3847/1538-4357/aaab52)
- Samsing, J., D’Orazio, D. J., Kremer, K., Rodriguez, C. L., & Askar, A. 2020a, *Physical Review D*, 101, 123010, doi: [10.1103/PhysRevD.101.123010](https://doi.org/10.1103/PhysRevD.101.123010)
- Samsing, J., MacLeod, M., & Ramirez-Ruiz, E. 2014, *The Astrophysical Journal*, 784, 71, doi: [10.1088/0004-637X/784/1/71](https://doi.org/10.1088/0004-637X/784/1/71)
- Samsing, J., & Ramirez-Ruiz, E. 2017, *The Astrophysical Journal Letters*, 840, L14, doi: [10.3847/2041-8213/aa6f0b](https://doi.org/10.3847/2041-8213/aa6f0b)
- Samsing, J., Bartos, I., D’Orazio, D. J., et al. 2020b, arXiv e-prints. <https://arxiv.org/abs/2010.09765>
- Sasaki, M., Suyama, T., Tanaka, T., & Yokoyama, S. 2018, *Classical and Quantum Gravity*, 35, 063001, doi: [10.1088/1361-6382/aaa7b4](https://doi.org/10.1088/1361-6382/aaa7b4)
- Silsbee, K., & Tremaine, S. 2017, *The Astrophysical Journal*, 836, 1, doi: [10.3847/1538-4357/aa5729](https://doi.org/10.3847/1538-4357/aa5729)
- Spruit, H. C. 1999, *Astronomy and Astrophysics*, 349, 189. <https://arxiv.org/abs/9907138>
- . 2002, *Astronomy & Astrophysics*, 381, 923, doi: [10.1051/0004-6361](https://doi.org/10.1051/0004-6361)
- Stephan, A. P., Naoz, S., Ghez, A. M., et al. 2019, *The Astrophysical Journal*, 878, 58, doi: [10.3847/1538-4357/ab1e4d](https://doi.org/10.3847/1538-4357/ab1e4d)
- Stone, N. C., Metzger, B. D., & Haiman, Z. 2017, *Monthly Notices of the Royal Astronomical Society*, 464, 946, doi: [10.1093/mnras/stw2260](https://doi.org/10.1093/mnras/stw2260)
- Strader, J., Chomiuk, L., MacCarone, T. J., Miller-Jones, J. C., & Seth, A. C. 2012, *Nature*, 490, 71, doi: [10.1038/nature11490](https://doi.org/10.1038/nature11490)
- Tagawa, H., Kocsis, B., Haiman, Z., et al. 2021, *The Astrophysical Journal*, 907, L20, doi: [10.3847/2041-8213/abd4d3](https://doi.org/10.3847/2041-8213/abd4d3)
- Takatsy, J., Bécsy, B., & Raffai, P. 2019, *Monthly Notices of the Royal Astronomical Society*, 486, 570, doi: [10.1093/mnras/stz820](https://doi.org/10.1093/mnras/stz820)
- Tiwari, V., Klimenko, S., Christensen, N., et al. 2016, *Physical Review D*, 93, 1, doi: [10.1103/PhysRevD.93.043007](https://doi.org/10.1103/PhysRevD.93.043007)
- Usman, S. A., Nitz, A. H., Harry, I. W., et al. 2016, *Classical and Quantum Gravity*, 33, 215004, doi: [10.1088/0264-9381/33/21/215004](https://doi.org/10.1088/0264-9381/33/21/215004)
- Van Der Walt, S., Colbert, S. C., & Varoquaux, G. 2011, *Computing in Science and Engineering*, 13, 22, doi: [10.1109/MCSE.2011.37](https://doi.org/10.1109/MCSE.2011.37)
- Virtanen, P., Gommers, R., Oliphant, T. E., et al. 2020, *Nature Methods*, 17, 261, doi: [10.1038/s41592-019-0686-2](https://doi.org/10.1038/s41592-019-0686-2)
- Wang, L., Spurzem, R., Aarseth, S., et al. 2016, *Monthly Notices of the Royal Astronomical Society*, 458, 1450, doi: [10.1093/mnras/stw274](https://doi.org/10.1093/mnras/stw274)
- Weatherford, N. C., Chatterjee, S., Kremer, K., & Rasio, F. A. 2020, *The Astrophysical Journal*, 898, 162, doi: [10.3847/1538-4357/ab9f98](https://doi.org/10.3847/1538-4357/ab9f98)
- Wen, L. 2003, *The Astrophysical Journal*, 598, 419, doi: [10.1086/378794](https://doi.org/10.1086/378794)
- Wong, K. W. K., Franciolini, G., Luca, V. D., et al. 2021, *Physical Review D*, 103, 23026, doi: [10.1103/PhysRevD.103.023026](https://doi.org/10.1103/PhysRevD.103.023026)
- Zevin, M., Samsing, J., Rodriguez, C., Haster, C.-J., & Ramirez-Ruiz, E. 2019, *The Astrophysical Journal*, 871, 15, doi: [10.3847/1538-4357/aaf6ec](https://doi.org/10.3847/1538-4357/aaf6ec)
- Zevin, M., Bavera, S. S., Berry, C. P., et al. 2021, *The Astrophysical Journal*, 910, 152, doi: [10.3847/1538-4357/abe40e](https://doi.org/10.3847/1538-4357/abe40e)